Doping Effects on Optical Properties of Low Temperature Grown ZnO Nanorod Arrays

O. Lupan[*,**], I. Tiginyanu[***], V. Ursaki[***] and L. Chow[*]

[*]Department of Physics, University of Central Florida, PO Box 162385
Orlando, FL 32816-2385, USA, lupan@physics.ucf.edu chow@physics.ucf.edu
[**]Department of Microelectronics and Semiconductor Devices, Technical University of Moldova, Republic of Moldova, lupan@mail.utm.md
[***] Laboratory of Nanotechnology, Institute of Electronic Engineering and Nanotechnologies, Academy of Sciences of Moldova, MD-2028, and National Center for Materials Study and Testing, Technical University of Moldova, MD-2004, Chisinau, Republic of Moldova, tiginyanu@asm.md

ABSTRACT

In this work, we explore the influence of Ag dopant concentration on the structural and optical properties of ZnO nanorods synthesized by hydrothermal technique. We present original results of a systematic investigation of crystal quality, morphology and photoluminescence properties by using X-ray diffraction (XRD), energy dispersive X-ray spectroscopy (EDX), scanning electron microscopy (SEM) and photoluminescence (PL). Strong effects of doping in Ag-doped ZnO nanorod arrays on optical properties are observed. The main advantage of the proposed synthesis is its simplicity and fast growth rates. The strength of the proposed nanotechnology is that any substrate can be used to grow doped ZnO nanorods and transferable nanorods.

Keywords: ZnO, nanorods, doping

1 INTRODUCTION

Over the last few years, ZnO nanorod arrays have been extensively investigated due to their potential for the development of novel nanodevices [1-3]. Usually undoped ZnO exhibits *n*-type conductivity ascribed to asymmetric doping limitations [4] and propensity to defects or impurities [5]. *P*-type conductivity of ZnO films has been achieved as a result of doping by N, As, Li, P, Sb, and Ag [4-7]. It is common that doping of zinc oxide often induces dramatic changes in its electrical and optical properties, which can be used in different useful applications. Some of these applications require both *p*- and *n*-type high quality nanostructures of ZnO.

The main motivation of this work is the absence of systematic studies of impurity doping using aqueous solution method. Even though, the solubility product constant of a chemical reaction usually ensures a stoichiometric product. Under suitable chemical environment, impurity doping through aqueous solution is possible. The improvement of the doped ZnO nanorods quality and the simplification of growth techniques are also important reasons to investigate aqueous solution method for doping ZnO. It is well known that *p*-type doping in ZnO is very difficult to achieve. Most of the proposed techniques employ catalysts or templates which may bring additional impurities into final nanomaterials, which will influence the purity, electrical and optical properties. Thus, the synthesis of ZnO nanorods at low-cost requires facile and low-temperature approaches which is important for nanodevice applications.

Here, we report on the influence of Ag dopant concentration on the structural, chemical, and optical properties of ZnO nanorods synthesized by hydrothermal technique. Strong effects of doping in Ag-doped ZnO nanorod arrays on optical properties will be presented. The experimental results are compared with theoretical data. In particular, the width of the band tails and the dependence of the FWHM of the PL band on carrier concentration were calculated using the model for broadening of impurity bands in heavily doped semiconductors developed by Morgan [8].

2 EXPERIMENTAL

2.1 Synthesis

All the chemical reagents used in our experiments were of analytical grade and without further purification. Si (100) wafers were used as a substrate for the fabrication of the ZnO nanorods. Substrates were cleaned as reported before [6,9]. In a typical procedure, zinc sulfate [$Zn(SO_4)\cdot 7H_2O$] was first dissolved into 50 ml of deionized water and then 25 ml (29.32%) of ammonia (NH_4OH) was added and stirred for 10 min to mix completely at room temperature. First set of pure ZnO nanorods (#1) samples was synthesized using 0.1-0.25 M of $Zn(SO_4)\cdot 7H_2O$. Second set of samples (#2) was prepared using 0.1-0.25 M of $Zn(SO_4)\cdot 7H_2O$ and 0.001-0.005 M of silver nitrate $Ag(NO_3)$ (99.7%) which was dissolved in 50 ml DI–water. An ammonia solution (29.6%) was added.

Subsequently, the resulting aqueous solution is poured into a 120 ml reactor. The vessels is placed on a preheated oven for 15 min at 96 °C and then allowed to cool down to room temperature for 30 min [1,10]. The main advantage of the proposed synthesis is its simplicity and fast growth rates (15 min versus several hours reported by previous researchers using aqueous synthesis methods or other techniques) [10].

One route for ZnO crystal growth by aqueous solution deposition can be described as follows [1,10]:

$$ZnSO_4 + 2NH_4OH \rightarrow Zn(OH)_2 + (NH_4)_2SO_4 \rightarrow$$
$$\rightarrow ZnO_s + 4NH_3(aq) + 2H_2O(l) \qquad (1)$$

The growth of ZnO nanorods in aqueous solution takes place when the temperature increases. In our experiment, ZnO nanocrystals were formed at a pH value of 10-11.

After the reaction was completed the grown ZnO nanorods on the substrates were rinsed in deionized water for 2 min and then the samples were dried in air at 150 °C for 5 min. Manipulation and reactions were carried out in air inside a fumehood.

2.2 Characterization techniques

The samples with pure and doped ZnO nanorods were analyzed by X-ray diffraction (XRD) using a Rigaku 'DB/MAX' powder diffractometer with a nickel-filtered Cu K_α radiation source (λ=1.54178 Å). The size and morphology of the samples with ZnO nanorods were explored using a VEGA TESCAN TS 5130MM scanning electron microscope (SEM) equipped with an Oxford Instruments INCA energy dispersive X-ray (EDX) system.

The photoluminescence was excited by the 351.1 nm line of an Ar^+ SpectraPhysics laser and analyzed in a quasi-backscattering geometry through a double spectrometer with 1200 grooves/mm gratings assuring a linear dispersion of 0.8 nm/mm. The spectral resolution was better than 0.5 meV. The samples were mounted on the cold station of a LTS-22-C-330 workhorse-type optical cryogenic system. The Raman scattering was investigated at room temperature with a MonoVista CRS Confocal Laser Raman System in the backscattering geometry under the excitation by a 532 nm DPSS laser.

3 RESULTS AND DISCUSSIONS

In order to examine the surface morphology and for measurement of the rod sizes, SEM has been used. Figure 1(a) shows the SEM images of undoped ZnO arrays formed from hexagonal rods on Si/SiO_2 substrate grown by hydrothermal technique. The synthesis of ZnO nanostructures is based on solution chemistry which involves different competing kinetics as well as growth regimes [1,10]. It can be seen in Figure 1(b) that a high density of about 200 nm nanowires grows over the entire surface of the substrate. The average length of the nanowires is about 1-2 μm.

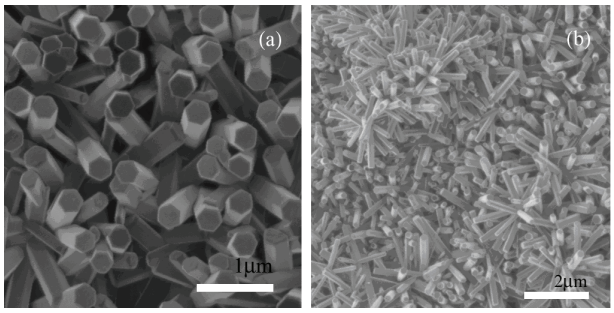

Figure 1: SEM images of the ZnO nanorod arrays on Si/SiO_2 substrate grown by hydrothermal technique: (a) undoped and (b) Ag-doped.

According to our experimental results, the nanorods obtained by our process can be easily transferred to other substrates and handled by Focuse Ion Beam (FIB) fabrication of nanodevices [1-3,10].

The Ag/Zn ratios in material were analyzed by EDX measurement and we found a linear correlation in the investigated range 0-3 %. The Ag/Zn ratios surveyed are 1/99 and 3/97 (at.%) in different scanned regions on samples (1) and (3), respectively.

X-ray diffraction was used to investigate the changes of phase structure and crystallite size of the ZnO nanorods. Fig. 2 shows the XRD patterns of pure and Ag-doped ZnO nanorods, which demonstrates that the all ZnO nanorods are with wurtzite structure [10].

Fig. 2a shows the XRD pattern recorded in the range of 30-70° with a scanning step of 0.02° of pure ZnO nanorods. It can be seen that all diffraction peaks are caused by crystalline ZnO with the hexagonal wurtzite structure (space group: $P6_3mc$(186); a = 0.3249 nm, c = 0.5206 nm).

The data are in agreement with the Joint Committee on Powder Diffraction Standards (JCPDS) card for ZnO (JCPDS 036-1451). It should be pointed out that a minute peak of silver or Ag_2O was found. No characteristic peaks of impurity phases such as Zn, S or $Zn(OH)_2$ or new phases were observed and no diffraction peaks except ZnO were found, which indicates that only single-phase hexagonal ZnO is present. This means that the impurity does not change the wurtzite structure of ZnO.

In Figure 2 the strongest detected (*hkl*) peaks are at 2θ values of 31.79°, 34.42°, 36.25°, 47.51°, 56.62°, and 62.83°, corresponding to the following lattice planes: (100), (002), (101), (102), (110), (103), respectively. In Fig. 2b there was a 0.20° shift to a lower 2θ angle value of the XRD diffraction peaks for Ag-doped ZnO nanorods as compared with those of pure ZnO nanorods. This can suggest that the most Ag atoms were in the ZnO lattice and conducted to distortion of the crystalline structure [6].

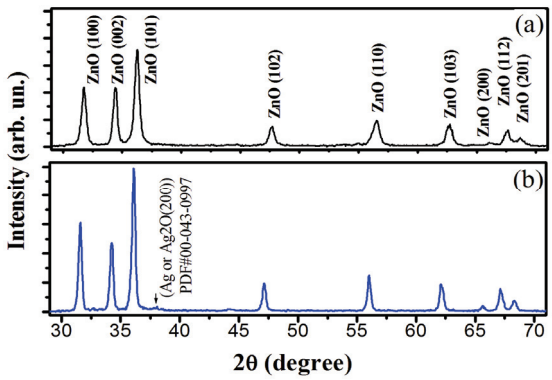

Figure 2: XRD patterns of the ZnO nanorods: (a) undoped and (b) Ag-doped.

The reason can be explained due to the fact that the radius of Ag^{1+} ion is greater than that of Zn^{2+} and Ag ions were substituted into zinc site and expand the lattice parameter in the Ag-doped ZnO nanorods.

The lattice constant *a* was calculated by

$$a = \frac{\lambda}{\sqrt{3}\sin\theta} \tag{2}$$

for the (002) orientation at $2\theta = 34.42°$, the lattice constant *c* was calculated by

$$c = \frac{\lambda}{\sin\theta} \tag{3}$$

The lattice constants *a* and *c* were determined as $a = 0.3250$ nm, $c = 0.5210$ nm for pure ZnO.

A small increase in the lattice parameters *a* and *c* (3.270 Å and 5.239 Å, respectively) would be expected when Zn^{2+} ions are replaced by Ag^{1+} ions because of the larger radius of Ag^{+} ions (0.126 nm) than Zn^{2+} ions (0.074 nm). The increase in the lattice parameters must be caused by either interstitial incorporation of Ag^{+} ions into the lattice or substitution of Zn ion.

Figure 3 presents the photoluminescence spectra (at 10 K) of ZnO nanorod arrays doped with 1.5 %, 3 %, and 4 % concentration of Ag. The spectra consist of resonant Raman scattering lines superimposed on a broad asymmetric PL band. It was previously shown that this PL band is mainly due to direct transitions of electrons between the conduction to valence band tails [11-13]. The broadening of the PL band is caused by the broadening of the band edges due to the potential fluctuations induced by the high concentration of intrinsic defects and impurities. The width of the band tails, and the dependence of the FWHM of the PL band on carrier concentration were calculated using the model for broadening of impurity bands in heavily doped semiconductors developed by Morgan [8]. With increasing the concentration of Ag from low to medium values the PL band is shifted from 3.28 eV to 3.34 eV, and the FWHM decreases from 180 meV to 100 meV. Further increase of the Ag concentration to the high value leads to the total quenching of the PL band.

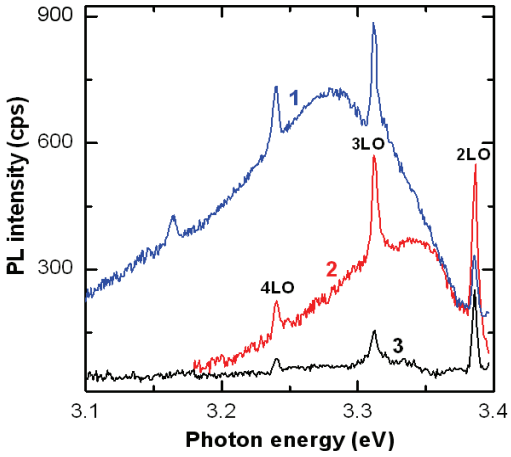

Figure 3: The PL spectra of ZnO nanorods doped with 1.5 % (1), 3 % (2) and 4 % (3) concentration of Ag. The spectra are measured at 10 K.

The shift of the PL band to higher energies and its narrowing indicates on the decrease of the potential fluctuations due to diminution of the concentration of donor defects, i. e. doping with Ag leads to the compensation of the *n*-type conductivity. The analysis of the resonant Raman scattering lines suggests the outgoing regime for samples doped with low and moderate concentration of Ag, where the 3LO RRS line is in resonance with the PL band. In contrast to this, the resonant Raman scattering is incoming for samples doped with high concentration of Ag. The ratio of the 3LO to the 2LO RRS lines intensity decreases from 2 to 1 with increasing the Ag concentration from low to medium, while this ratio is 0.5 for samples with high Ag concentration.

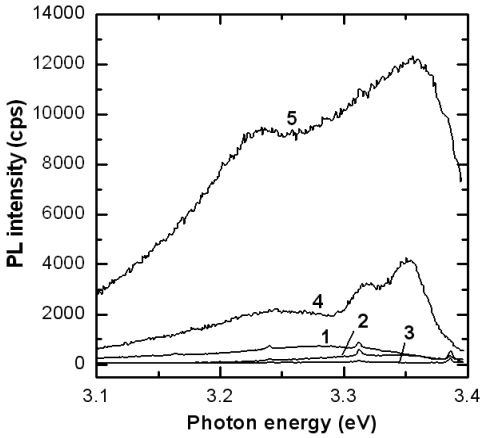

Figure 4: The PL spectra of ZnO nanorods doped with Sn (4) and In (5) as compared to samples doped with Ag (1-3). The spectra are measured at 10 K.

In contrast to Ag doping, doping with Sn and In leads to the increase of the intensity of the PL band related to donor impurities (Figure 4). The complex character of the PL band in this case indicates on the complex distribution of the donor impurity states.

According to our preliminary data, device-quality *p-n* nanorods-based *p-n* junctions can be fabricated using the nanotechnology involved. It is anticipated that the ZnO nanorods will find many applications in novel nanodevices [1-3,6,10,14] and the design of some original device structures is proposed.

4 CONCLUSIONS

Pure and Ag-doped ZnO nanorods were successfully synthesized through a facile hydrothermal route. ZnO nanorods are found to have high crystal quality. Each individual ZnO rod showed a hexagonal basis.

X-ray diffraction, scanning electron microscopy and photoluminescence have been used to characterize the structure, morphology and chemical composition of the samples. The zinc oxide rods synthesized were found to be of single-crystal nature with hexagonal wurtzite structure and stoichiometric ZnO composition. XRD measurements indicate that the synthesized ZnO crystals are in the hexagonal phase and well-aligned parallel to the [0001] crystal direction.

From XRD results have been calculated lattice constants *a* and *c* for Ag-doped ZnO nanorods. With the doping concentration of 3%, the lattice constant *a* increases linearly from 3.250 to 3.269 Å, and *c* increases linearly from 5.210 to 5.239 Å.

The analysis of the near bandgap PL band suggests that a decrease of potential fluctuations occurs with increasing the concentration of the doped Ag due to decrease of the concentration of donor defects, i. e. doping with Ag leads to the compensation of the *n*-type conductivity.

Acknowledgments Dr. Chow acknowledges financial support by the National Science Foundation (Award # 0901361). Partial financial support from US Department of Agriculture award #58-3148-8-175 is also acknowledged. Dr. Lupan acknowledges financial support for post-doctoral position in Professor Chow's group. The research described here was made possible in part by an Award for young researchers OL (MTFP-1014B Follow-on) from the Moldovan Research and Development Association (MRDA) under funding from the U.S. Civilian Research & Development Foundation (CRDF).

REFERENCES

[1] O. Lupan, L. Chow and G. Chai, "Novel hydrogen gas sensor based on single ZnO nanorod," Microelectronic Eng. 85, 2220, 2008.

[2] O. Lupan, G. Chai and L. Chow, "Fabrication of ZnO nanorod-based hydrogen gas nanosensor," Microelectronics Journal. 38, 1211, 2007.

[3] G. Chai, O. Lupan, L. Chow and H. Heinrich, "Crossed zinc oxide nanorods for ultraviolet radiation detection," Sensors & Actuators: A. Physical. 150, 184, 2009.

[4] S. B. Zhang, S. H. Wei and A. Zunger, "Intrinsic *n*-type versus *p*-type doping asymmetry and the defect physics of ZnO," Phys. Rev. 63, 075205, 2001.

[5] A. Gulino and I. Fragala, "Deposition and Characterization of Transparent Thin Films of Zinc Oxide Doped with Bi and Sb," Chem. Mater. 14, 116, 2002.

[6] O. Lupan L. Chow, L. K. Ono, B. Roldan Cuenya, G. Chai, H. Khallaf, S. Park and A. Schulte, "Synthesis and Characterization of Ag- or Sb-doped ZnO Nanorods by a Facile Hydrothermal Route," J. Phys. Chem. C. under review, 2010.

[7] S. Limpijumnong, S. B. Zhang, S. H. Wei, C. H. Park, Phys. Rev. Lett. 92, 155504, 2004.

[8] T. N. Morgan, Phys. Rev. 139, A343, 1965.

[9] S.T. Shishiyanu, O.I. Lupan, T.S. Shishiyanu, V.P. Şontea and S.K. Railean, Electrochimica Acta 49, 4433, 2004.

[10] O. Lupan, L. Chow, G. Chai, B. Roldan, A. Naitabdi, A. Sculte, H. Heinrich, " Nanofabrication and characterization of ZnO nanorod arrays and branched microrods by aqueous solution route and rapid thermal processing," Mater. Sci. Eng.: B. 145, 57, 2007.

[11] V.V. Ursaki, O.I. Lupan, L. Chow, I.M. Tiginyanu, V.V. Zalamai, "Rapid thermal annealing induced change of the mechanism of multiphonon resonant Raman scattering from ZnO nanorods," Solid State Commun. 143, 437, 2007.

[12] V.V. Ursaki, I.M. Tiginyanu, V.V. Zalamai, E.V. Rusu, G.A. Emelchenko, V.M. Masalov, E.N. Samarov, "Multiphonon resonant Raman scattering in ZnO crystals and nanostructured layers," Phys. Rev. B 70, 155204, 2004.

[13] V.V. Zalamai, V.V. Ursaki, R.V. Rusu, P. Arabadji, I.M. Tiginyanu, L. Sirbu, "Photoluminescence and resonant Raman scattering in highly conductive ZnO layers," Appl. Phys. Lett. 84, 5168, 2004.

[14] G. Chai, E. Rusu, L. Chow, G. Stratan, H. Heinrich, S. Park, A. Schulte, O. Lupan, V.Trofim, S.Railean, "Microsensor on single ZnO microwire," The 2009 International Semiconductor Conference, October 12-14, 2009, Sinaia, Romania, vol. 2. pp.287-290.